Steering Vehicle Control by Switched Model Predictive Control

S. Di Cairano [*] **H.E. Tseng** [*] **D. Bernardini** [**]
Alberto Bemporad [***]

[*] *Powertrain Control R&A, Ford Motor Co., Dearborn, MI, US*
[**] *Dip. Ing. dell'Informazione, Università di Siena, Italy*
[***] *Dep. Mechanical and Structural Eng., Università di Trento, Italy*

Abstract: We propose a switching Model Predictive Control (MPC) strategy to control vehicle steering by actuating active front steering (AFS) and electronic stability control (ESC). After describing the piecewise affine prediction model used for MPC design, where the nonlinearities arise from the relation between sideslip angles and tire forces, a switching MPC strategy is implemented, where different local MPC controllers are used depending on the current tire force conditions. The designed controller maintains most of the benefits of a previously designed hybrid model predictive controller, but it has lower complexity and allows more flexible design. The controller stability is verified and the controller behavior during challenging step steering maneuvers is tested in closed-loop simulations against a nonlinear vehicle model.

1. INTRODUCTION

Electronic Stability Control (ESC) (Koibuchi et al. (1996)) and Active Front Steering (AFS) (Ackermann (1997)) have been proven successful in improving vehicle stability and as a consequence in reducing single vehicle accidents (see for instance Koibuchi et al. (1996); Ackermann (1997); Ono et al. (1994); Tøndel and Johansen (2005) and the references therein).

Further advantages can be obtained by coordinating the two actuators using advanced control strategies (Ono et al. (1994)). Model predictive control (MPC) (Bemporad et al. (2002b)) is a candidate for optimizing actuator coordination while accounting for physical and specification constraints.

In recent years, MPC has been successfully applied to problems related to vehicle dynamics and handling (Falcone et al. (2007); Bernardini et al. (2009)). In Falcone et al. (2007) a linear time-varying MPC was proposed for coordination of active steering and braking in an autonomous vehicle navigating along a known trajectory. In Bernardini et al. (2009) a hybrid model predictive control approach was applied to the case of vehicle trajectory stabilization on unknown trajectories. However, both the approaches are too computationally demanding for current ECU implementations.

Starting from the results of Bernardini et al. (2009), we propose a switched model predictive controller that maintains most of the hybrid MPC, while reducing the control law complexity, hence resulting in a controller that can be implemented in currently available ECUs. Switched MPC approaches have been previously applied in automotive (Ortner and Del Re (2007); Bemporad et al. (2007); Stewart and Borrelli (2008); Di Cairano et al. (2010)), and they prove to be particularly advantageous for this application due to the selected prediction model.

In the proposed approach, a set of local MPC laws are designed with switching logics derived from the system physics. The stability of the closed-loop system is verified by using the explicitly computed control law (Bemporad et al. (2002b)), and simulations results are shown in Section 4. The conclusions and future research directions are summarized in Section 5.

Notation: We avoid to explicitly show the dependence in time of the variables, when not needed. For a matrix A, $'$ indicates transpose, and $[A]^{(m)}$ indicates the m^{th} column. Inequalities between vectors are intended componentwise. For a discrete-time vector $a(k)$ $a(h|k)$ is the predicted value of $a(k+h)$ basing on data at sampling instant k.

2. VEHICLE STEERING MODEL

We consider a vehicle equipped with AFS and ESC implemented by differential braking. For modeling the vehicle dynamics in high speed turns [1] we use the bicycle model shown in Figure 1, as suggested by Gillespie (1992).

We consider a reference frame that moves with the vehicle. The frame origin is at the vehicle center of mass, with the x-axis along the longitudinal vehicle direction pointing forward, the y-axis pointing to the left side of the vehicle, and the z-axis pointing upwards. We focus on the dynamics on the xy-plane, where, the angles increase counterclockwise. The tire sideslip angle (or simply slip angles) is the angle between the tire direction and the velocity vector at the tire. In the bicycle model, α_f [rad] and α_r [rad] are the tire sideslip angles at the front and at the rear tires, respectively. According to the chosen reference frame, the front and rear slip angles in Figure 1 are negative.

Since the longitudinal component of the velocity at the wheels is assumed equal to the one at the center of mass

[1] Turns that are performed in normal "on-road" driving are referred to as *high speed* turns (Gillespie (1992)).

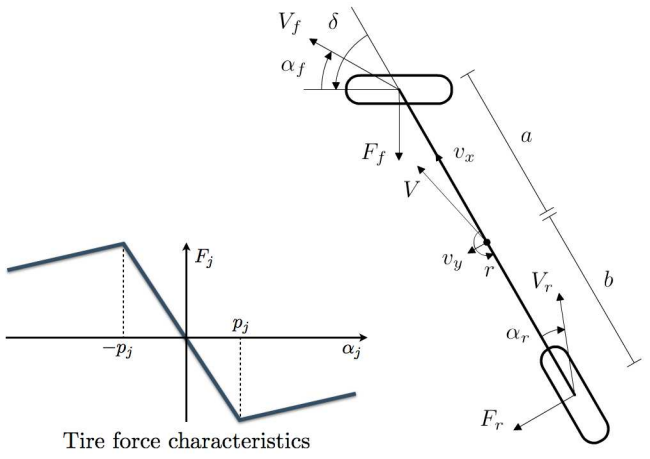

Fig. 1. Schematics of the bicycle model of the vehicle, and qualitative characteristic of the sideslip angle-tire force relation.

v_x [m/s], and the lateral velocity at the wheels is computed by adding to the lateral velocity at the center of mass v_y [m/s] the contribution due to the rotation,

$$\tan(\alpha_f + \delta) = \frac{v_y + ar}{v_x}, \quad \tan\alpha_r = \frac{v_y - br}{v_x}, \tag{1}$$

where a [m] and b [m] are the distances of the front and rear wheel axes from the vehicle center of mass, respectively, δ [rad] is the total steering angle (i.e., the sum of the driver steering with the additional AFS steering), and r [rad/s] is the yaw rate. The front and rear tire forces F_f [N], F_r [N], respectively, are nonlinear functions of α_f, α_r and of the longitudinal slip [2] $\sigma \in [0,1]$. We consider an approximated model of the tire forces that, for a constant longitudinal slip σ, is piecewise linear

$$F_j(\alpha_j) = \begin{cases} d_j(\alpha_j + p_j) - e_j & \text{if} \quad \alpha_j < -p_j \\ c_j\alpha_j & \text{if} \quad -p_j \le \alpha_j \le p_j \\ d_j(\alpha_j - p_j) + e_j & \text{if} \quad \alpha_j > p_j \ , \end{cases} \tag{2}$$

where $j \in \{f, r\}$, $j = r$ indicates rear tires, and $j = f$ indicates front tires, p_j [rad] is called *critical slip angle*, and c_j [N/rad], d_j [N/rad], e_j [N] are usually identified from experimental data. Three regions of operations per pair of tires are considered, negative saturation ($\alpha_j < -p_j$), linear ($|\alpha_j| \le p_j$) and positive saturation ($\alpha_j > p_j$). A qualitative sideslip angle-tire force characteristic is shown in the lower left corner of Figure 1. It is obvious from (2) that the tire forces are symmetric functions, i.e., for any $j \in \{f, r\}$ and α_j, $F_j(-\alpha_j) = -F_j(\alpha_j)$.

The tire slip angles are small for high speed turns (Gillespie (1992)), hence (1) is approximated by

$$\alpha_f = \frac{v_y + ar}{v_x} - \delta, \quad \alpha_r = \frac{v_y - br}{v_x} \ . \tag{3}$$

By differentiating (3) and assuming a constant longitudinal velocity v_x during the maneuver,

$$\dot\alpha_f = \frac{\dot v_y + a\dot r}{v_x} - \dot\delta, \quad \dot\alpha_r = \frac{\dot v_y - b\dot r}{v_x} \ . \tag{4}$$

From (3), $\alpha_f - \alpha_r = \frac{v_y + ar}{v_x} - \delta - \frac{v_y - br}{v_x}$, hence

$$r = \frac{v_x}{a+b}(\alpha_f - \alpha_r + \delta) \ . \tag{5}$$

[2] The longitudinal slip is the normalized difference between the wheel axle velocity and the velocity at the wheel.

For constant v_x, the vehicle acceleration is decomposed into the acceleration of a frame rotating with constant yaw rate r, and the lateral acceleration at the center of mass. Since the only forces on the vehicle are F_f and F_r,

$$\dot v_y = \frac{F_f\cos\delta + F_r}{m} - rv_x \ . \tag{6}$$

The yaw acceleration is computed as

$$\dot r = \frac{aF_f\cos\delta - bF_r + Y}{I_z} \ , \tag{7}$$

where I_z [kg m^2] is the vehicle mass moment of inertia with respect to the center of mass, and Y [Nm] is the yaw moment applied by differential braking. For small steering angles, $\cos\delta \simeq 1$, hence substituting (5), (6) and (7) into (4), and neglecting the contribution of $\dot\delta$,

$$\begin{aligned} \dot\alpha_f &= \tfrac{F_f+F_r}{mv_x} - \tfrac{v_x}{a+b}(\alpha_f - \alpha_r + \delta) + \tfrac{a}{v_x I_z}(aF_f - bF_r + Y), \\ \dot\alpha_r &= \tfrac{F_f+F_r}{mv_x} - \tfrac{v_x}{a+b}(\alpha_f - \alpha_r + \delta) - \tfrac{b}{v_x I_z}(aF_f - bF_r + Y). \end{aligned} \tag{8}$$

The dynamics model (2), (5), (8) is a second order piecewise affine (PWA) system (Sontag (1981))

$$\dot x(t) = A_i^c x(t) + B_i^c u(t) + \phi_i^c \tag{9a}$$

$$y(t) = C^c x(t) + D^c u(t) \tag{9b}$$

$$i \in \mathcal{I} \ : \ H_i x(t) \le K_i \tag{9c}$$

where $x = [\alpha_f \ \alpha_r]'$ is the state vector, $u = [Y \ \delta]'$ is the input vector, $y = r$ is the output, and $i \in \mathcal{I}$ is the active region, where $\mathcal{I} = \{1, \dots, s\}$ and s is the number of regions of the PWA system. Inequalities (9c) are derived from the inequalities in (2), and partition the state space into polyhedral regions, that define the different operating conditions (linear, and positive and negative saturation, for each pair of tires). Hence, they are also called system modes. The matrices A_i, B_i, $i \in \mathcal{I}$, C, D, define the vehicle dynamics in the different conditions, and are obtained by substituting the different force expressions (2) in (8). The active region (or active mode) i of the PWA system is selected by evaluating (9c) for the current value of the state x, i.e., the sideslip angles.

Since (2) defines 3 conditions per each pair of tires, there are in total 9 modes. Since (8) is symmetric with respect to α_f and α_r due to the symmetry of (2) and the polyhedral partition is symmetric, the PWA vector field in (9a) is symmetric with respect to the state-input vector.

3. SWITCHED MODEL PREDICTIVE CONTROL DESIGN

The piecewise affine model developed in Section 2 is discretized in time with sampling period T_s

$$x(k+1) = A_i x(k) + B_i u(k) + \phi_i \ , \tag{10a}$$

$$y(k) = Cx(k) + Du(k) \ , \tag{10b}$$

$$i \ : \ H_i x(k) \le K_i \ , \tag{10c}$$

obtaining a model that can be used to design a hybrid MPC controller for tracking a reference yaw rate r_r by actuating the active front steering and the differential braking. The design of such a controller has been explored by the authors in (Bernardini et al. (2009)). The hybrid MPC controller solves at every control cycle the problem

$$\min_{U_N(k)} \quad J(x(k), U_N(k), r_r) \tag{11a}$$
$$\text{s.t.} \quad x(0|k) = x(k) \tag{11b}$$
$$i(h|k) \quad : \quad H_{i(h|k)}x(h|k) \leq K_{i(h|k)}, \tag{11c}$$
$$x(h+1|k) = \quad A_{i(h|k)}x(h|k) + B_{i(h|k)}u(h|k) + \phi_{i(h|k)} \tag{11d}$$
$$y(k) = Cx(k) + Du(k) \ , \tag{11e}$$
$$u_{\min} \leq \ u(h|k) \leq u_{\max} \tag{11f}$$
$$x_{\min} \leq \ x(h|k) \leq x_{\max} \tag{11g}$$
$$y_{\min} \leq \ y(h|k) \leq y_{\max} \tag{11h}$$
$$h = 0, \ldots, N-1$$

where J is the (quadratic) cost function that encodes the control objective (yaw rate tracking, actuators usage, etc.), (11f),(11g),(11h) model the constraints on inputs, states, and outputs, N is the prediction horizon and $U_N(k) = \{u(0|k), \ldots, u(N-1|k))\}$. Optimization problem (11) can be formulated as a mixed-integer quadratic program where the integer variables are used to select the system modes. Although satisfactory performance is achieved, the computational burden of mixed-integer programming is too large for implementation in automotive microcontrollers. Even if synthesized in explicit MPC form by multiparametric mixed integer quadratic programming (mpMIQP) (Bemporad et al. (2002a)), the controller is still too complex in terms of memory occupancy and worst case computations required.

The large complexity of the explicit hybrid MPC is due to the fact that a PWA control law is computed for each region sequence along the prediction horizon. For m modes and horizon N, m^N control laws are computed, that cannot be merged into a single piecewise affine function (Bemporad et al. (2002a)). Thus, the m^N laws must be stored together with their value functions, that describe the minimum of J as a function of the state x for each control law. At each control cycle, all the m^N laws are evaluated for the current value of x and the one with smaller value function is selected. Symmetry can be used to reduce the modes to 4, and by choosing horizon $N = 3$, 64 PWA control laws are obtained, for a total of more than 2000 PWA regions.

However, it was verified in simulations that the system in closed-loop with the hybrid MPC controller exhibits relatively few mode switches, and that almost no multiple switches occur over short horizons (0.5s–1s). As a consequence, one can consider as prediction model PWA system (10) where the mode is maintained constant and the constraints that define the PWA region are ignored after the first step. Thus, (11c) is enforced only for $h = 0$, and $i(h|k) = i(0|k)$ for all $h = 1, \ldots, N-1$. This reduces the feasible mode sequences to m, even though the effects of the mode switches during the prediction horizon are neglected. Furthermore, due to (10c), for any given $x(k)$, only one $i(0|k) \in \mathcal{I}$ exists such that (11c) is satisfied for $h = 0$, hence the active mode can be computed before the optimization problem is solved. Let

$$\gamma_{\text{MPC}}(i, x(k)), \ i \in \mathcal{I} \tag{12}$$

be the MPC control law obtained by (11) where $i(h|k) = \bar{\imath}$ for all $h = 0, \ldots, N-1$, and (11c) is removed. The switched model predictive control algorithm is defined as follows. Given $x(k)$, (i) find i such that $H_i x(k) \leq K_i$, (ii) select as command $u(k) = \gamma_{\text{MPC}}(i, x(k))$. Due to the modifications to (11), for any fixed $i \in \mathcal{I}$ (12) is a piecewise affine function that can be computed by multiparametric programming (Bemporad et al. (2002b)). Since for a fixed $i \in \mathcal{I}$ (12) is applied only at the states x such that $H_i x \leq K_i$, we call it *local MPC law.*

Remark 1. The PWA polyhedral partition (10c) does not depend on the input $u(k)$. Thus, given $x(k)$ there is only one feasible mode $\bar{\imath} \in \mathcal{I}$, and a single MPC law has to be evaluated. In the case of general PWA partitions, $H_i x(k) + J_i u(k) \leq K_i$, multiple MPC laws might need to be evaluated. Thus, (11) where (11c) is enforced only for $h = 0$ and $i(h|k) = i(0|k)$ for all $h = 1, \ldots, N-1$ is solved for all $i(0|k) \in \mathcal{I}$, obtaining several input commands and optimum costs. The control input to be applied is selected as the one that provides the smallest cost. However, the solution of m QPs is in general simpler than the solution of MIQP (11) modeling m^N mode sequences.

3.1 Local MPC law design

We describe now the formulation and computation of $\gamma_{\text{MPC}}(i, x)$, $i \in \mathcal{I}$ that are used in the switched MPC design. Since each local MPC law is a linear MPC more degrees of freedom with respect to the hybrid MPC design can be exploited.

The selection of the cost function and of the MPC decision variables is guided by the problem specifications. The objective is to track the desired vehicle yaw rate, which is generated from the driver command on the steering wheel and current driving conditions. Hence, the tracking error, $|y(k) - r_r(k)|$ is accounted for in the cost function.

Since differential braking perturbs the longitudinal vehicle dynamics and might give a negative feeling to the driver, in stationary conditions the yaw moment should be 0, and the steering angle should converge to the value that generates the desired yaw rate. As a consequence, the selected decision variables are the yaw moment Y obtained by differential braking, and the steering angle variation $\Delta\delta(k) = \delta(k) - \delta(k-1)$. The active front steering angle to be applied at time k is $\delta(k) = \delta(k-1) + \Delta\delta(k)$, where $\delta(k-1)$ is an additional state in the prediction model.

Finally, in order to improve vehicle stability, weights on the sideslip angles are also added. The resulting cost function is

$$J = \sum_{k=0}^{N-1} q_r(y(k) - r_r(k))^2 + q_Y Y(k)^2 + q_\delta \Delta\delta(k) + q_{\alpha_f}\alpha_f(k)^2 + q_{\alpha_r}\alpha_r(k)^2, \tag{13}$$

where $q_r \geq 0$ is the tracking weight, $q_Y > 0$ is the yaw moment actuator weight, $q_\delta > 0$ is the total steering angle rate of change weight, and $q_{\alpha_f} \geq 0$, $q_{\alpha_r} \geq 0$ are the weights on the front and rear tire slip angles, respectively.

Let $\delta_\infty(r)$ be the steering angle such that the vehicle yaw rate in steady state is equal to r when no yaw moment is applied. By (13), if $q_r > 0$, $q_{\alpha_f} = 0$, $q_{\alpha_r} = 0$ and the system is in stationary conditions ($\alpha_j(k) = \alpha_j(k-1)$, $j \in \{f, r\}$), $y(k-1) = r_r$ and $\delta(k-1) = \delta_\infty(r)$, the cost associated

to the control sequence $\delta(h|k) = \delta_\infty(r)$, $Y(h|k) = 0$ for all $h = 0, \dots, N-1$ is 0 and is the optimum, since (13) is nonnegative. On the other hand, by setting $q_{\alpha_f} > 0$, $q_{\alpha_r} > 0$ and $q_r = 0$ the controller minimizes the sideslip angles.

The first behavior ($q_{\alpha_f} = q_{\alpha_r} = 0$) is applied in the linear tire region to track the desired yaw rate. The second one ($q_{\alpha_f}, q_{\alpha_r} > 0$) is used in the saturated tire regions. In these regions if the same cost for the linear region were used, the controller would try to increase the steering effort as a reaction to a decreased yaw rate reference, due to the tire force characteristics (2). This would cause the slip angles to increase to the point where little tire force is available, ultimately causing loss of stability. By applying weights on the angles, the controller tries to steer the vehicle in the linear region, instead.

In the case of unfeasible references, the control law will be switching on the border of the linear region, and the actuator weights can be used to control the switching frequency. The oscillations in the yaw moment and steering angle, that can be also reduced by changing weights in the cost function, have the beneficial side effect of indicating to the driver that the vehicle is reaching the maximum achievable yaw rate, hence the action on the steering wheel should be reduced.

Let us define the extended prediction model $x_p(k+1) = A_i^p x_p(k) + B_i^p u_p(k)$ where

$$x_p(k) = \begin{bmatrix} x(k) \\ \phi(k) \\ \delta(k-1) \\ r_r(k) \\ \varepsilon(k-1) \end{bmatrix}, \; A_i^p = \begin{bmatrix} A_i & I & [B_i]^{(2)} & 0\ 0 \\ 0 & I & 0 & 0\ 0 \\ 0 & 0 & 1 & 0\ 0 \\ 0 & 0 & 0 & 1\ 0 \\ C_i & 0 & [D_i]^{(2)} & -1\ 0 \end{bmatrix}, \; B_i^p = \begin{bmatrix} B_i \\ 0 \\ [0\ 1] \\ 0 \\ D_i \end{bmatrix}$$

$u_p(k) = [Y(k) \; \Delta\delta(k)]$, $\phi(k)$ models the affine term in (10a), and $\varepsilon(k) = y(k) - r_r(k)$ is the tracking error at time k.

Thus, for $i \in \mathcal{I}$, the i^{th} local MPC problem is

$$\min_{U_N(k)} \sum_{h=0}^{N-1} x_p(h|k)' Q x_p(h|k) + u_p(h|k)' R u_p(h|k) \quad (14a)$$

$$\text{s.t. } x_p(h+1|k) = A_i^p x_p(h|k) + B_i^p u(h|k), \quad (14b)$$

$$u_{\min} \le u_p(h_c|k) \le u_{\max}, \;\; {\scriptstyle h_c=0,\dots,N_c-1} \quad (14c)$$

$$x_{\min} \le x_p(h_y|k) \le x_{\max}, \;\; {\scriptstyle h_y=1,\dots,N_y} \quad (14d)$$

$$u_p(h_b|k) = u_p(N_c-1|k), \; {\scriptstyle h_b=N_c,\dots,N} \quad (14e)$$

$$x_p(0|k) = \left[x(k)' \;\; \phi(0|k)' \;\; \delta(k-1) \;\; r(k) \;\; \varepsilon(k) \right]', \quad (14f)$$

the cost function matrices Q, R are used to formulate (13), and (14c), (14d), are the constraints on inputs and states, which include limits on the slip angles, limits on the steering actuation, and limits on the differential braking yaw moment,

$$|\alpha_j| \le \bar{\alpha}_j, \; j \in \{f, r\}, \; |Y| \le \bar{Y}, \; |\delta| \le \bar{\delta}.$$

N is the prediction horizon, $N_c \le N$ is the control horizon, the number of free control moves, and $N_y \le N$ is the constraint horizon, the number of steps along which state and output constraints are enforced. Problem (14) is a quadratic problem (QP), whose complexity can be reduced by selecting N_c, N_y smaller than N.

The solution of (14) is precomputed by multiparametric programming with respect to the parameter vector in x_p, that contains $x(k)$, $\delta(k-1)$, $\phi(k)$, $r_r(k)$. The resulting i^{th} local MPC law is a piecewise affine function

$$\gamma_{\text{MPC}}(i, x_p) = F_j^i x_p + G_j^i \quad (15)$$

$$j : H_j^i x_p \le K_j^i \quad (16)$$

where $j \in \mathcal{J}_i$, $\mathcal{J}_i = \{1, \dots, s_i\}$, and s_i is the number of regions of the i^{th} local MPC law.

By using the symmetry of the dynamics and the fact that at positive and negative saturation the tire force equations differ only for their affine term (ϕ_i), since $\phi(k)$ is included in $x_p(k)$, only 4 local control laws are used, modeling linear and saturated behavior for front and rear axis. Negative and positive saturation are differentiated by the affine term, $\phi(k)$, which is now maintained constant along the prediction horizon.

At time step k:
1. find $i \in \mathcal{I}$ such that $H_i x(k) \le K_i$.
2. find $j \in \mathcal{J}_i$ such that $H_j^i x(k) \le K_j^i$
3. compute $u(k) = F_j^i x(k) + G_j^i$.

Algorithm 1. Switched model predictive control.

The online execution of the switched MPC algorithm is summarized in Algorithm 1, where at step 1 the currently active MPC law is selected, at step 2, the active region of the explicit MPC law selected at step 1 is found, and at step 3 the input is computed basing on the affine gain associated to the active region of the active controller.

The complete control law obtained by the switched MPC is the piecewise affine system

$$u = F_j^i x(k) + G_j^i \quad (17a)$$

$$\text{if } : \; H_i x(k) \le K_i \quad (17b)$$

$$H_j^i x(k) \le K_j^i \quad (17c)$$

where (17b) is the controller selection rule and (17c) is the region selection rule. As a consequence, the closed loop system is the piecewise affine system

$$x(k+1) = (A_i^p + B_i^p F_j^i) x(k) + G_j^i \quad (18a)$$

$$\text{if } : \; H_i x(k) \le K_i \quad (18b)$$

$$H_j^i x(k) \le K_j^i \quad (18c)$$

whose stability can be studied locally and globally via the techniques discussed in (Di Cairano et al. (2008)).

4. SIMULATION RESULTS

In this section we show the simulation results for the MPC controller in closed loop with the nonlinear model of the vehicle dynamics which, besides the nonlinearities on the yaw rate and on the tire forces, also includes a model of the steering actuation dynamics. However, the tire force curves and the friction coefficient of the simulation model match the one of the prediction model. The nonlinear simulation model will not be described here in details, due to space limitations. We consider $m = 1891\text{kg}$, $I_z = 3213\text{kgm}^2$,

$a = 1.47$m, $b = 1.43$m, consistent with a typical passenger vehicle, and nominal $v_x = 20$m/s. The parameters of the piecewise affine model of the tire forces are assumed $c_f = -9.06 \cdot 10^4$ $d_f = 9.06 \cdot 10^3$, $e_f = -9.14 \cdot 10^3$ for the front tires, where the critical slip angle is $p_f = 0.11$rad, and $c_r = -1.65 \cdot 10^5$, $d_r = 1.65 \cdot 10^4$, $e_r = -9.39 \cdot 10^3$ for the rear tires, with critical slip angle $p_r = 0.06$rad.

The switched MPC controller is implemented with sampling period $T_s = 100$ms, and the horizons are $N = 9$ steps for prediction, $N_c = 3$ steps for control, and $N_y = 3$ steps for constraints. The input constraints in (14c) are

$$-0.35 \leq \delta \leq 0.35 \text{ [rad]}, \quad -1000 \leq Y \leq 1000 \text{ [Nm]},$$

the state constraints in (14d), which are due to the limited knowledge of the tire force maps, are

$$-0.2 \leq \alpha_f \leq 0.2 \text{ [rad]}, \quad -0.12 \leq \alpha_r \leq 0.12 \text{ [rad]}.$$

We have tuned the weights to trade off between tracking performance, robustness to the model approximations, and reduced switching frequency on the border of the linear region. We have selected $q_r = 1$, $q_{\alpha_f} = 0$, $q_{\alpha_r} = 0$ for the linear region local MPC, $q_r = 0$, $q_{\alpha_f} = 0.1$, $q_{\alpha_r} = 1$ for all the other regions, for simplicity. The weights on the inputs are $q_Y = 10^{-8}$, $q_\delta = 10$ for all the local MPC, where the large difference in the yaw moment weight is related to its wide operating range. The local MPC controllers are synthesized in explicit form (14) and the switching conditions are added. The worst case number of operations (sums, products, comparisons) per control cycle is 10^4, without any code optimization. This amounts to a worst case of 10^5 operations per second, feasible for automotive ECUs. Thus, although the complexity of the control law can be reduced, we did not pursue further simplifications.

Using the explicit control law, we have verified that the closed loop is asymptotically stable at the origin ($\alpha_r = 0$, $\alpha_f = 0$, $r_r = 0$) where the maximum eigenvalue absolute value is 0.491. Since the open-loop dynamics in the saturated tires regions are unstable and the actuators are limited, there are regions where the closed-loop dynamics are unstable. However, by extensive simulation we verified that the closed-loop unstable regions are not reached when starting from within the linear region.

The reference yaw rate r_r is generated, without loss of generality, by a static map of the steering wheel position and longitudinal velocity.

The simulations focus on aggressive maneuvers, where r_r changes abruptly as a square wave. In Figure 2 the case where the desired yaw rate changes between -0.35rad/s and 0.35rad/s every 5s is shown. Figure 2(a) shows that the controller regulates the vehicle yaw rate on the reference, and that the yaw moment provided by differential braking is used during the transient, but it is zero at steady state, as required. From Figure 2(b) it can be observed that during this simulations the tire forces are in the linear region, which means that only one local MPC controller is used. In Figure 3 the case of a reference switching between -0.55rad/s and 0.55rad/s every 5s is shown. Due to the tire force limits, the maximum available lateral acceleration is not enough to achieve this yaw rate, and the controller stabilizes the system on a close steady state achievable yaw rate, see Figure 3(a). In order to stabilize

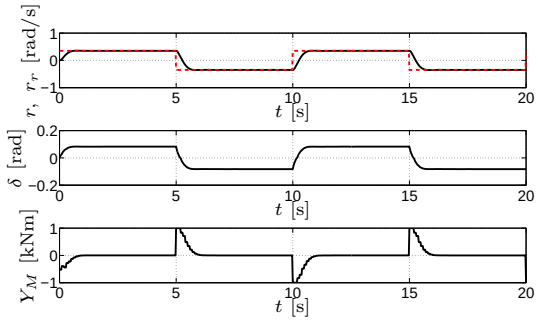

(a) Upper plot: Yaw rate (solid) and reference yaw rate (dashed). Center plot: steering angle. Lower plot: Yaw moment from ESC.

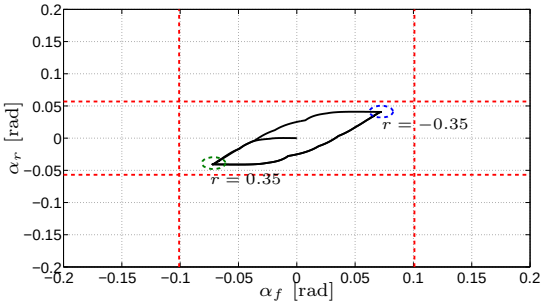

(b) Sideslip angles phase plane, the tire force regions boundaries are shown (dashed)

Fig. 2. Simulation of achievable yaw rate reference tracking

the system, a (light) action of the ESC is applied also during stationary conditions. In Figure 4 we see that in the same conditions an open-loop control that actuates the steering angle proportionally to the desired yaw rate, becomes unstable and cause the vehicle to spin.

Preliminary experimental results of the controller implemented in a test vehicles are shown in Figure 5, for a slalom maneuver. The controller action is consistent with the simulation results, achieving the feasible target yaw rates, and countersteering in the unachievable ones. The countersteering action is more aggressive than in simulation, due to the imperfect tire modelling, inconstant friction coefficient, and changing longitudinal velocity.

5. FUTURE DIRECTIONS AND CONCLUSIONS

We have proposed a switched model predictive controller for vehicle steering dynamics. The controller is based on a piecewise affine vehicle steering model, and the resulting MPC law complexity is reduced with respect to a hybrid MPC controller hence allowing implementation in vehicle ECUs. The switched MPC controller achieves convergence to the desired yaw rate when this is feasible, otherwise drives the steering dynamics to a close feasible yaw rate.

REFERENCES

Ackermann, J. (1997). Robust control preventing car skidding. *Control Systems Magazine*, 17(3), 23–31.

Bemporad, A., Borrelli, F., and Morari, M. (2002a). On the optimal control law for linear discrete time hybrid systems. In *Hybrid Systems: Computation and Control*, volume 2289 of *Lec. Not. in Computer Science*, 105–119. Springer-Verlag.

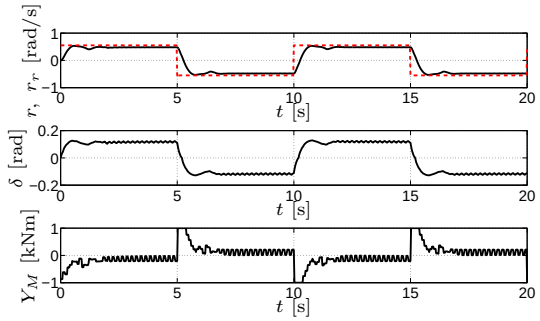

(a) Upper plot: Yaw rate (solid) and reference yaw rate (dashed). Center plot: steering angle. Lower plot: Yaw moment from ESC.

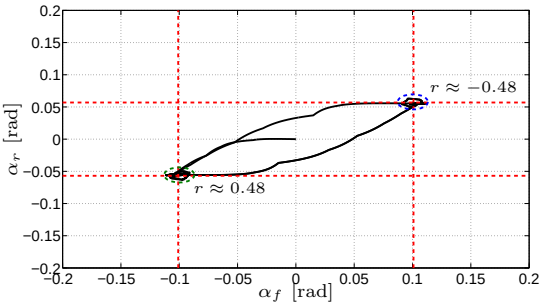

(b) Sideslip angles phase plane, the tire force regions are shown (dashed)

Fig. 3. Simulation of unachievable yaw rate reference tracking

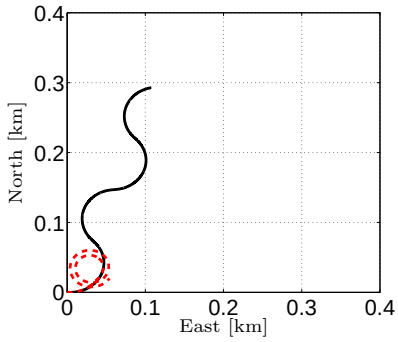

Fig. 4. Vehicle position during the second simulation: closed-loop (solid) and open-loop (dashed)

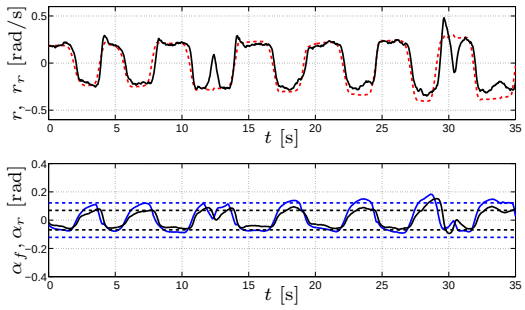

(a) Upper plot: Yaw rate reference (dashed) and yaw rate (solid). Lower plot: slip angles (solid) and saturation angles (dotted)

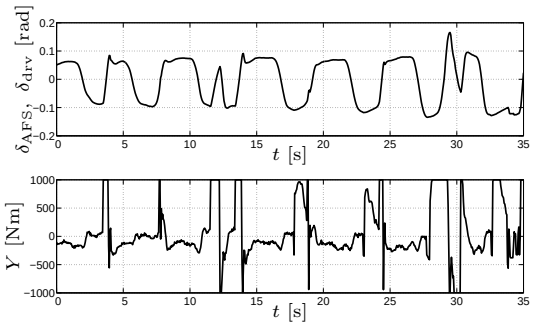

(b) Upper plot: driver steering angle (dashed) and AFS actuator steering angle (solid). Lower plot: differential braking yaw moment

Fig. 5. Slalom experimental test.

and Control, 5686–5691.

Di Cairano, S., Yanakiev, D., Bemporad, A., Kolmanovsky, I., and Hrovat, D. (2010). Model predictive powertrain control: an application to idle speed regulation. In *Lec. N. in Control and Inf. Science*, 402.

Falcone, P., Borrelli, F., Asgari, J., Tseng, H., and Hrovat, D. (2007). Predictive active steering control for autonomous vehicle systems. *IEEE Trans. Contr. Systems Technology*, 15(3), 566–580.

Gillespie, T. (1992). *Fundamentals of vehicle dynamics*. Society of Automotive Engineers, Inc.

Koibuchi, K., Masaki, Y., Fukada, Y., and Shoji, I. (1996). Vehicle stability control in limit cornering by active braking. SAE paper 960487.

Ono, E., Takanami, K., Iwama, N., Hayashi, Y., Hirano, Y., and Satoh, Y. (1994). Vehicle integrated control for steering and traction systems by μ-synthesis. *Automatica*, 30(11), 1639–1647.

Ortner, P. and Del Re, L. (2007). Predictive control of a diesel engine air path. *IEEE Trans. Contr. Systems Technology*, 15(3), 449–456.

Sontag, E. (1981). Nonlinear regulation: The piecewise linear approach. *IEEE Trans. Automatic Control*, 26(2), 346–358.

Stewart, G. and Borrelli, F. (2008). A Model Predictive Control Framework for Industrial Turbodiesel Engine Control. In *Proc. 48th IEEE Conf. on Decision and Control*, 5704–5711.

Tøndel, P. and Johansen, T. (2005). Control allocation for yaw stabilization in automotive vehicles using multiparametric nonlinear programming. In *Proc. American Contr. Conf.*, 453–458.